Hybrid Mesh Generation for NAL Experimental Airplane

Yasushi ITO* and Kazuhiro NAKAHASHI†
Tohoku University, Aoba-yama 01, Sendai 980-8579, JAPAN

ABSTRACT

An automated and robust unstructured hybrid mesh generation method comprised of tetrahedra, prisms, and pyramids has been developed. The hybrid grid generation starts with isotropic tetrahedral grids to enhance the robustness of the algorithm. The user-specified number of prismatic layers is then added keeping the mesh validity. The tetrahedra near no-slip walls are shifted inward and the resulting gap between the tetrahedra and the walls is filled up with prismatic elements step by step. The addition of prismatic elements is stopped if a local mesh has incorrect topology. The method is applied to the experimental supersonic airplane model designed at NAL. Computed results by solving the Navier-Stokes equations are compared with wind tunnel data and the validity of the method is demonstrated.

1. INTRODUCTION

Tetrahedral unstructured grids have become popular in Computational Fluid Dynamics (CFD) because they are flexible enough to treat three-dimensional complex geometries and have adaptive refinement/unrefinement capabilities. Owing to the recent developments of surface and volume grid generation methods, isotropic tetrahedral grids are easy to create and widely used to solve inviscid flows and low Reynolds number viscous flows around complex geometries.

For high Reynolds number viscous flows, however, the unstructured grid still has issues to be addressed. In order to resolve thin boundary layers on the solid surface accurately, a minimum grid spacing in the normal direction to the surface has to be very small, which causes a stiffness problem of the flow solver. Moreover, the generation of such anisotropic stretched grids near the wall is another issue.

To treat the high Reynolds number viscous flows by the unstructured grid, several methods of generating highly stretched grid on the surfaces have been proposed [1-10]. Some of them generate fully tetrahedral grids and the others create hybrid grids consisting of prismatic and tetrahedral elements. Although these methods have shown their capabilities in simulating viscous flows around 3D configurations, their reliability still needs to be improved in order to treat various configurations encountered in engineering applications [11].

The authors proposed an automated and robust unstructured hybrid mesh generation method based on isotropic tetrahedral grids [12]. The method started with isotropic tetrahedral grid generation for the entire computational domain. The tetrahedra near no-slip walls were shifted gradually to accommodate each prismatic layer. By using the initial isotropic tetrahedral mesh as a background grid for the hybrid mesh generation, mesh quality control may be easier. Prisms were then added near the walls keeping the mesh validity. The addition was locally stopped if negative volume elements were created, and pyramidal or tetrahedral elements filled the gap.

In this paper, the hybrid mesh generation method is applied to the NAL experimental supersonic airplane model and the resulting flow computations are shown in comparison with experiment.

2. GRID GENERATION METHOD

Figure 1 shows the outline of the hybrid mesh generation process.

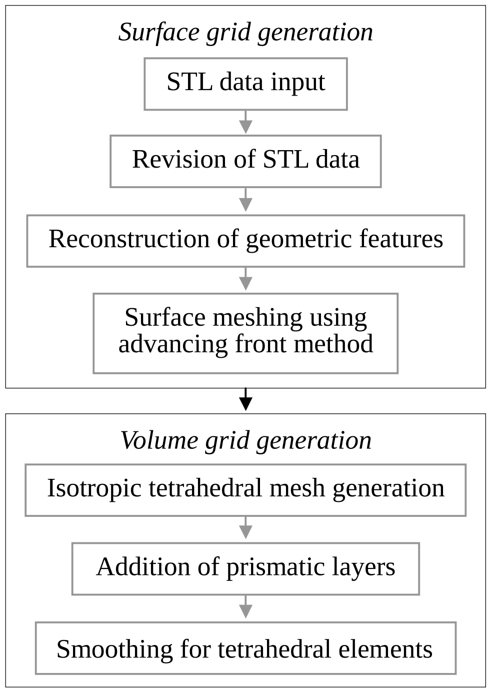

Fig. 1 Outline of grid generation process

2.1. Surface Grid

CAD stereolithography (STL) files are employed for the surface definition. The STL file format is *de facto*

* Graduate student, Dept. of Aeronautics and Space Engineering
† Professor, Dept. of Aeronautics and Space Engineering

standard in rapid prototyping, and its defined tessellated model is precise enough to use CFD grid generation. The direct advancing front method based on geometric features is employed to generate a surface grid [13]. This method is efficient and effective to generate fine surface meshes and have been demonstrated for various complex geometries [14].

2.2. Volume Grid

The entire computational domain defined by the surface mesh is tessellated by isotropic tetrahedra [15]. Nowadays, techniques to generate unstructured grid has been well developed and any computational field about complex shapes can be automatically filled up with isotropic tetrahedral cells.

Prismatic layers are then added on the solid surface. The detailed process is discussed in Ref. 12. The generation of each prismatic layer is continued until the user specified number of layers is obtained. User inputs to generate prismatic layers are only three parameters: the number of the layers, an initial layer thickness near boundary wall, and a stretching factor. No user intervention is required during the process. From the isotropic tetrahedral mesh, each prismatic layer is added. First, the tetrahedra near no-slip walls are shifted in order to accommodate a prismatic layer. Second, the resulting space is checked. If there is locally not enough space to add prisms or negative volume elements are created, the addition of prisms is stopped there.

3. FLOW SOLVER

The full Reynolds-averaged Navier-Stokes equations that retained the unsteady form were solved by a finite volume cell-vertex scheme. The Harten-Lax-van Leer-Einfeldt-Wada (HLLEW) Reimann solver [16] was used for the numerical flux computations. The Lower-Upper-Symmetric Gauss-Seidel (LU-SGS) implicit method [17] was used for time integration. A one-equation turbulence model by Goldberg and Ramakrishnan [18] was implemented to treat turbulent flows.

4. RESULT

The volume mesh used here consisted of 1,055,846 nodes, 1,536,764 tetrahedra, 1,520,363 prisms and 20,129 pyramids. Figure 2 shows the hybrid mesh. Parameters for generating prismatic layers were as follows: the number of layers was 20, the initial layer thickness corresponded with $0.05/\sqrt{\mathrm{Re}}$ and the stretching factor was 1.2. The mesh consisted of 1,055,846 nodes, 1,536,764 tetrahedra, 1,520,363 prisms, 20,129 pyramids, 100,934 boundary triangles, and 11,606 boundary quadrangles. The CPU time to add the prismatic layers to the original tetrahedral mesh was about 20 minutes on a PC with a 1 GHz Pentium III processor, having 512 MB of memory.

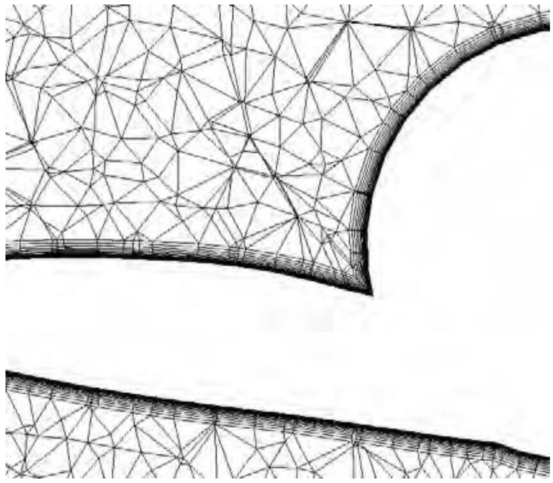

(a)

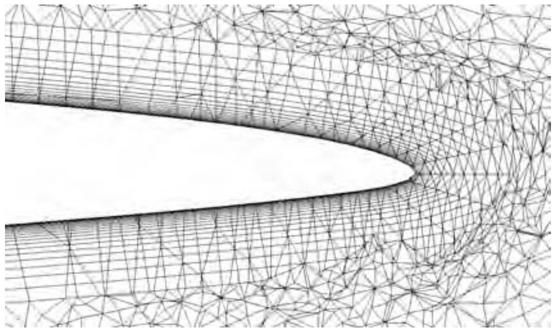

(b)

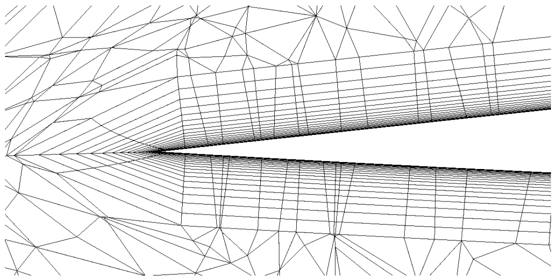

(c)

Fig. 2 Hybrid mesh: (a) cross-flow cross section at $x = 0.5l$; (b) spanwise cross section near the wing leading edge at 30% semi-span station; (c) the same section near the tailing edge

The Navier-Stokes equations were solved at a free-stream Mach number of 2.0, a unit Reynolds number based on meter of 27.5×10^6 and angles of attack from -2.0° to 6.0°. The CFD results were compared with the wind tunnel test data by NAL. They conducted wind tunnel tests using two different models: one was 8.5% scale full configuration model, and the other was 23.3% fuselage-wing configuration one. The latter model was tested in a different Reynolds number flow (a unit Reynolds number was 21.1×10^6 at a free-stream Mach number of 2.0). The wind tunnel test model had a sting at its tail; accordingly aerodynamic coefficients were evaluated except for the sting in both the wind tunnel test and the CFD post processing.

Figure 3 shows the lift curve, the drag polar and the pitching moment curve. The CFD result was compared with experiment using the 8.5% scale model. Although there were discrepancies in several drag counts at the low angle of attack region, good agreement was achieved. The chordwise pressure coefficient (C_p) distributions at 0%, 30 %, 50 % and 70 % semi-span stations are shown in Fig. 4 (0° angle of attack), Fig. 5 (2° angle of attack), and Fig. 6 (4° angle of attack). The distributions of the CFD result at the sharp corners such as the trailing edges of the wing and the vertical fin were not physically correct. The reason would come from the skewness of the prisms there as shown in Fig. 2d. This deficiency will be addressed in future.

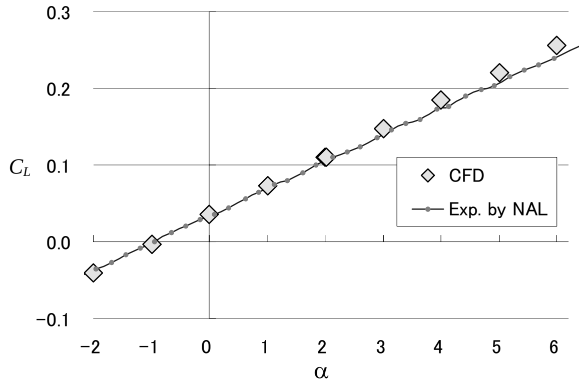

(a) Lift curve

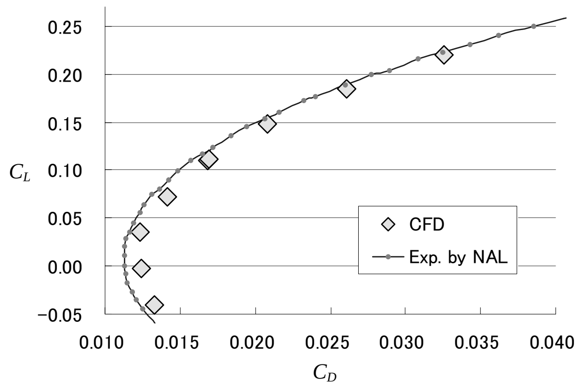

(b) Drag polar

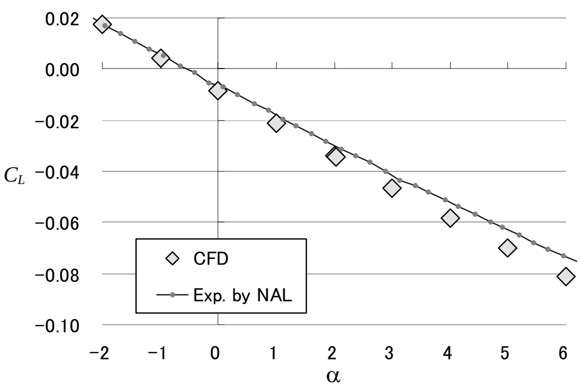

(c) Pitching moment curve

Fig. 3 Lift curve, drag polar and pitching moment curve for NAL experimental airplane (M_∞ = 2.0, Re = 27.5×10^6)

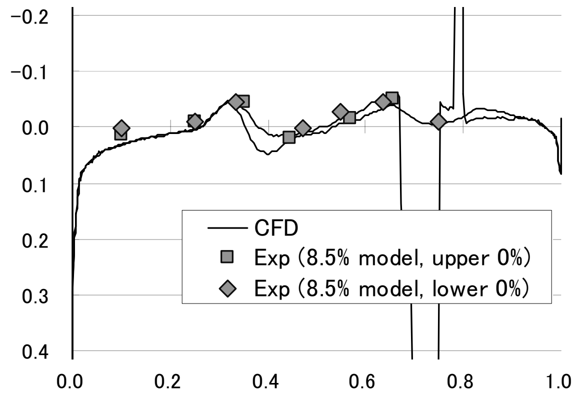

(a) 0 % semi-span station

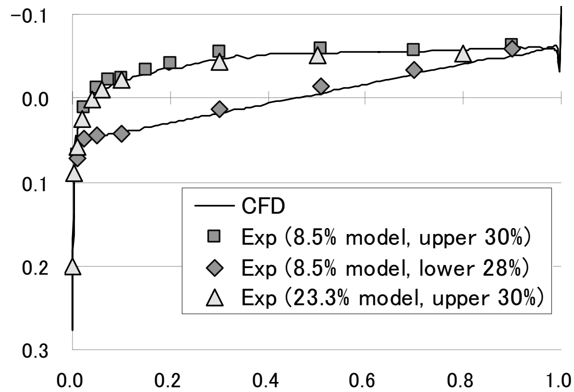

(b) 30 % semi-span station

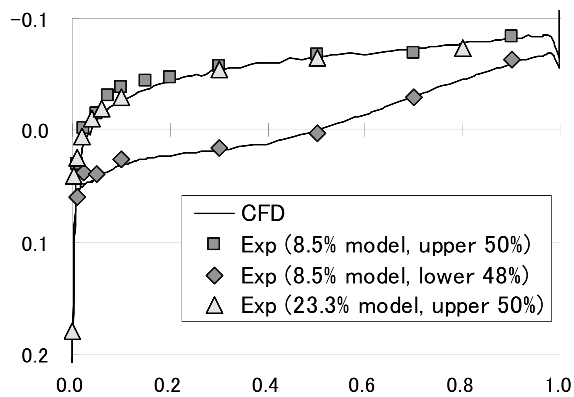

(c) 50 % semi-span station

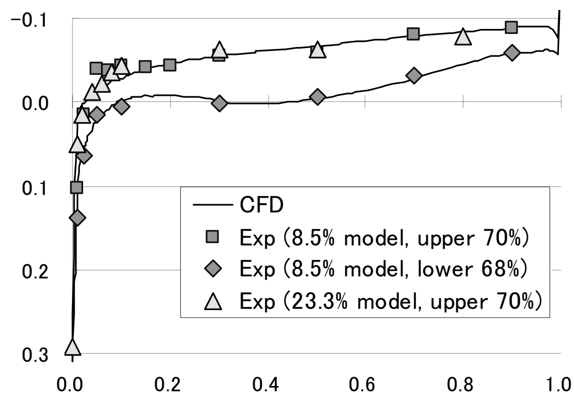

(d) 70 % semi-span station

Fig. 4 Cp distributions at 0° angle of attack

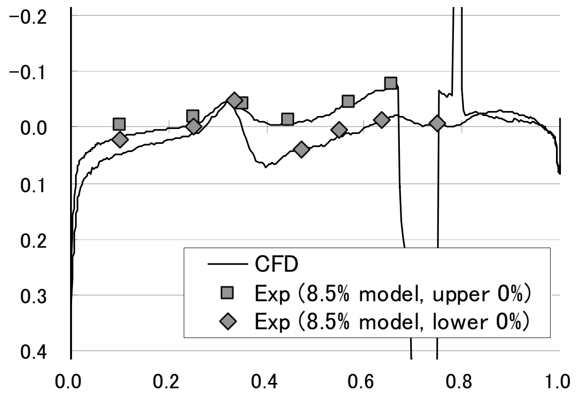

(a) 0 % semi-span station

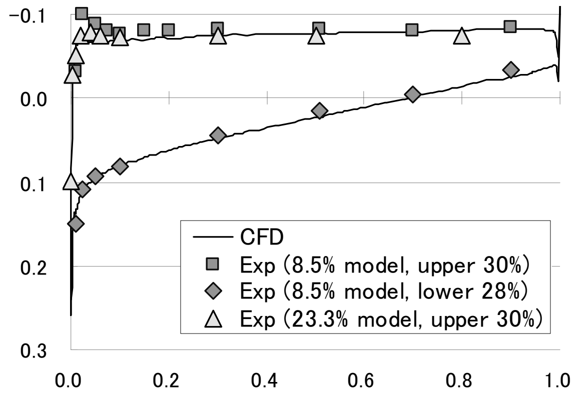

(b) 30 % semi-span station

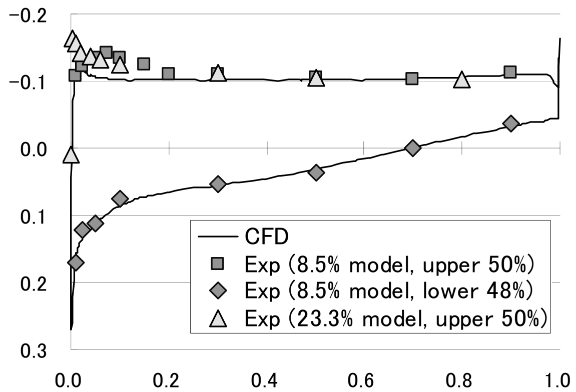

(c) 50 % semi-span station

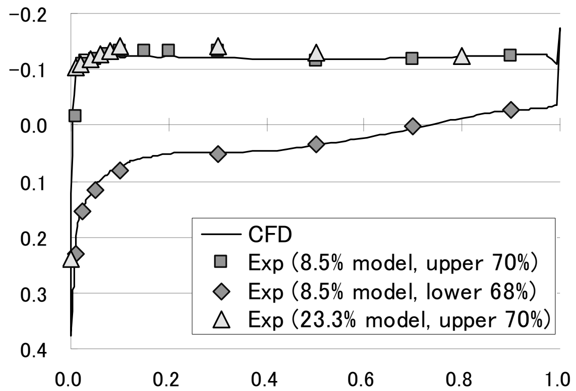

(d) 70 % semi-span station

Fig. 5 Cp distributions at 2° angle of attack

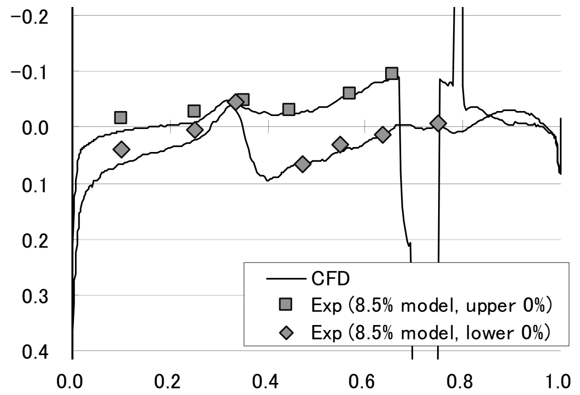

(a) 0 % semi-span station

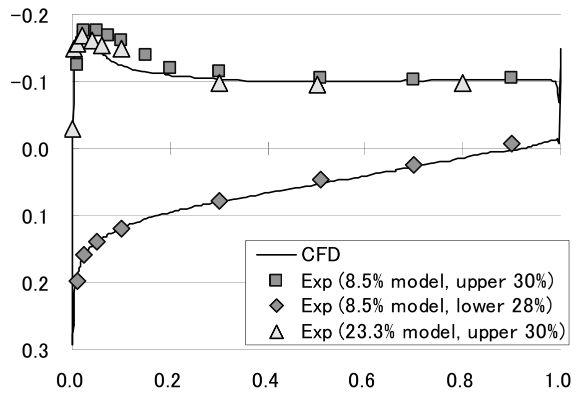

(b) 30 % semi-span station

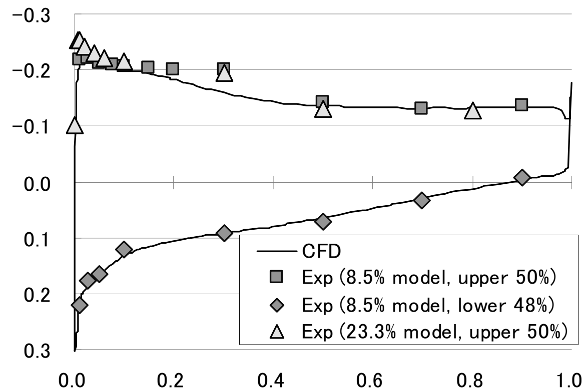

(c) 50 % semi-span station

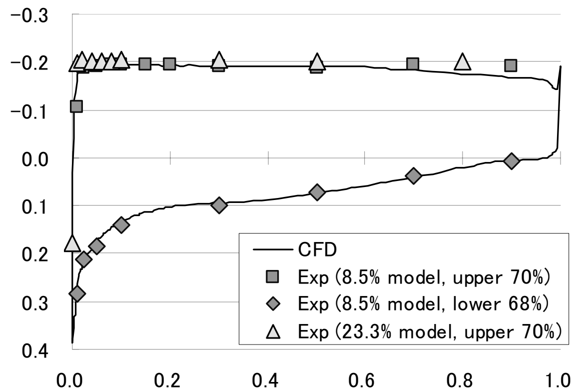

(d) 70 % semi-span station

Fig. 6 Cp distributions at 4° angle of attack

5. CONCLUSIONS

An automated hybrid grid generation method based on isotropic tetrahedral meshes has been developed. For the robustness, the hybrid grid generation method started from isotropic tetrahedral grids that can be generated for any complex geometries. Each prismatic layer was then added step by step near no-slip walls automatically. The method was applied to the NAL experimental airplane model. The computed results by solving the Navier-Stokes equations were compared with experiment. Although the mesh generation near sharp corners such as the wing trailing edge was not proper, almost good agreements of lift and drag coefficients were achieved. These certified that the proposal method practically generated well-qualified grid distribution for high Reynolds number viscous flow computations.

ACKNOWLEDGEMENTS

The authors would like to thank T. Fujita, a graduate student of Tohoku University, for his help in generating the STL data.

REFERENCES

1. Marcum, D. L., "Generation of Unstructured Grids for Viscous Flow Applications," AIAA Paper 95-0212, 1995.
2. Pirzadeh, S., "Three-Dimensional Unstructured Viscous Grids by the Advancing-Layers Method," *AIAA Journal*, Vol. 34, No. 1, 1996, pp. 43-49.
3. Hassan, O., Morgan, K., Probert, E. J. and Peraire, J., "Unstructured Tetrahedral Mesh Generation for Three-Dimensional Viscous Flows," *International Journal for Numerical Methods in Engineering*, Vol. 39, 1996, pp. 549-567.
4. Sharov, D. and Nakahashi, K., "Hybrid Prismatic/Tetrahedral Grid Generation for Viscous Flow Applications," *AIAA Journal*, Vol. 36, No. 2, 1998, pp. 157-162.
5. Khawaja, A. and Kallinderis, Y., "Hybrid Grid Generation for Turbomachinery and Aerospace Applications," *International Journal for Numerical Method in Engineering*, Vol. 49, 2000, pp. 145-166.
6. Garimella, R. V., and Shephard, M. S., "Boundary Layer Mesh Generation for Viscous Flow Simulations," *International Journal for Numerical Method in Engineering*, Vol. 49, 2000, pp. 193-218.
7. Michal, T., and Cary, A., "Unstructured Grid Extrusion for Viscous Flow Simulations," AIAA Paper 2001-0444, 2001.
8. Sharov, D., Luo, H., Baum, J. D. and Löhner, R., "Unstructured Navier-Stokes Grid Generation at Corners and Ridges," AIAA Paper 2001-2600, 2001.
9. Currie, T. C., "Modifying Isotropic Tetrahedral Grids for Viscous Simulations," Proceedings of the 7th Annual Conference of the Computational Fluid Dynamics Society of Canada, 1999.
10. Löhner, R. and Cebral, J., "Generation of non-isotropic unstructured grids via directional enrichment," *International Journal for Numerical Method in Engineering*, Vol. 49, 2000, pp. 219-232.
11. Wurtzler, K. E., Tomaro, R. F., and Witzeman, F. C., "Analysis of Three Unstructured Grid Techniques From a User's Perspective," Proceeding of the 7th International Conference on Numerical Grid Generation in Computational Field Simulations, 2000, pp.357-366.
12. Ito, Y. and Nakahashi, K., "Unstructured Hybrid Grid Generation Based on Isotropic Tetrahedral Grids," AIAA Paper 2002-0861, 2002.
13. Ito, Y. and Nakahashi, K., "Direct Surface Triangulation Using Stereolithography (STL) Data," *AIAA Journal*, Vol. 40, No. 3, 2002 (to be published). See also AIAA Paper 2000-0924, 2000.
14. Ito, Y. and Nakahashi, K., "Surface Triangulation for Non-trimmed Surface Models," AIAA Paper 2001-2601, 2001.
15. Sharov, D. and Nakahashi, K., "A Boundary Recovery Algorithm for Delaunay Tetrahedral Meshing," Proceedings of the 5th International Conference on Numerical Grid Generation in Computational Field Simulations, 1996, pp.229-238.
16. Obayashi, S. and Guruswamy, G. P., "Convergence Acceleration of an Aeroelastic Navier-Stokes Solver," *AIAA Journal*, Vol. 33, No. 6, 1995, pp. 1134-1141.
17. Sharov, D. and Nakahashi, K., "Reordering of Hybrid Unstructured Grids for Lower-Upper Symmetric Gauss-Seidel Computations," *AIAA Journal*, Vol. 36, No. 3, pp. 484-486, 1998.
18. Goldberg, U. C. and Ramakrishnan, S. V., "A Pointwise Version of Baldwin-Barth Turbulence Model," *Computational Fluid Dynamics*, Vol. 1, 1993, pp.321-338.